# Development and validation of a dual modality TREK-1 screening assay on the automated patch clamp Qube 384 platform

Alexander S Haworth[1], Steven A Trim[2], Emma L Veale[3], Edward B Stevens[1]

[1]Metrion Biosciences Ltd, Granta Centre, Granta Park, Cambridge, CB21 6AL, UK
[2]Venomtech Limited, Discovery Park Sandwich, Kent, CT13 9FE, UK
[3]Universities of Greenwich and Kent at Medway, Anson Building, Chatham, Kent, ME4 4TB, UK

## Introduction

Two-pore domain $K^+$ ($K_{2P}$) channels are a family of four-pass transmembrane $K^+$ channels that dimerise, as homomers or heteromers, to form a functional $K^+$ channel complex capable of regulating membrane potential through a background $K^+$ conductance. $K_{2P}$ channels have widespread tissue expression[1], and within the nervous system they play a key role in membrane hyperpolarisation and the regulation of neuronal excitability. Moreover, these channels are implicated in a range of neurological disorders[1,2], such as pain[3], depression[4], epilepsy[5], mental developmental disorders[5], and migraine[6], and therefore represent attractive drug targets for these conditions.

$K_{2P}$ channels are encoded by fifteen genes (KCNKx family) in mammals and can be divided into six subfamilies: TASK (TASK-1, TASK-3, TASK-5), THIK (THIK-1, THIK-2), TWIK (TWIK-1, TWIK-2, KCNK7), TREK (TREK-1, TREK-2, TRAAK), TALK (TASK-2, TALK-2, TALK-1) and TRESK[7,8]. $K_{2P}$ channels display outward rectification upon stimulation, except TWIK-1, which displays a conventional linear current-voltage response[9]. $K_{2P}$ channels do not possess a conventional S4 voltage-sensing domain and are instead gated by extracellular $K^+$ motility within the selectivity filter, with efflux promoting channel activation and influx promoting inactivation[9]. $K_{2P}$ channels exhibit a plethora of activating and inhibiting stimuli, such as intracellular and extracellular pH change[10], polyunsaturated fatty acids[10], membrane stretch[10], certain phospholipids[11,12], temperature[13], and general anaesthetics[14]. Certain stimuli can abolish $K_{2P}$ outward rectification, such as arachidonic acid stimulation of TREK-1[9]. Furthermore, $K_{2P}$ channels possess distinct pharmacology compared to other $K^+$ channels, with sensitivity to common anticonvulsants, antipsychotics, anaesthetics and antiarrhythmics but relative insensitivity to common $K^+$ blockers, such as 4-AP and TEA[15].

Despite $K_{2P}$ channels possessing a high degree of pharmacological promiscuity, they lack a toolkit of subtype-specific activators and inhibitors. Coupled with their fundamental role in regulating neuronal excitability and their implication in a range of neurological disorders, there is a necessity to develop robust assays to facilitate the drug discovery process. Here, we report the development and optimisation of a TREK-1 functional assay using the Qube 384, an automated patch clamp platform capable of supporting high-throughput screening. The assay was optimized to identify both activators and inhibitors on the same plate, providing key mechanistic data for high value, limited supply screening libraries such as venom fractions used in this study (Targeted Venom Discovery Array, T-VDA, Venomtech, UK).

## Results

TREK-1 is sensitive to a multitude of pharmacological and non-pharmacological stimuli that can potentiate and inhibit activity. These include TREK agonists, BL-1249[16] and GI-530159[17], which can significantly enhance current amplitude. TREK-1 current expression was verified following robust activation with BL-1249 (10 µM, Figure 1A, C) and GI-530159 (30 µM, Figure 1B, C) on the QPatch48 platform.

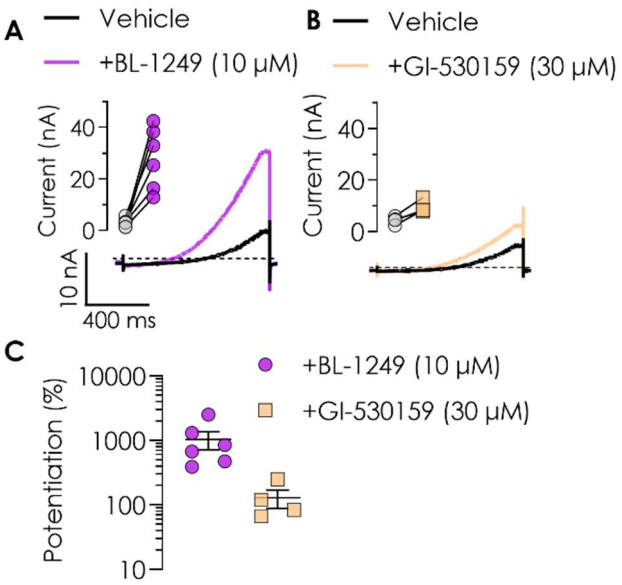


**Figure 1. QPatch48 validation of TREK-1 currents.** (**A, B**) Representative TREK-1 currents elicited by an 800 ms ramp from -100 mV to +60 mV in the presence and absence of BL-1249 (**A**, 10 µM) and GI-530159 (**B**, 30 µM), inserts represent potentiation in individual cells. The quantified % increase in TREK-1 current amplitude for both compounds at +60 mV (**C**). Recordings performed in multi-hole acquisition using a QPatch48 platform at 25°C. Data displayed as Mean ± SEM.

The TREK-1 assay required the ability to detect both agonist and antagonist activity, where a sufficient baseline current amplitude was necessary for screening antagonists. However, utilising BL-1249 or GI-530159 to enhance baseline current amplitude is not an optimal screening approach, as TREK-1 ligands may compete at the same binding site.

Temperature is a well-characterised modulator of TREK-1 activity[13]. Increasing temperature between 27.5°C and 35°C caused a dramatic increase in current amplitude from minimal to maximal response (Figure 2A).

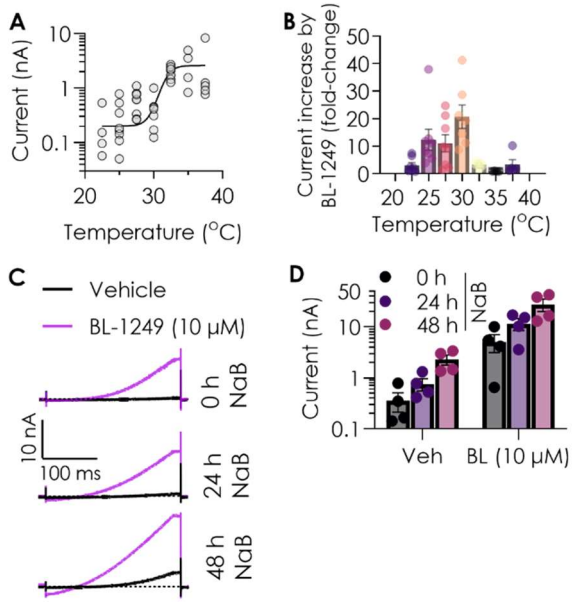


**Figure 2. Optimisation of TREK-1 parameters for dual screening of agonist and antagonist activity using a QPatch48.** (**A**) The effect of increasing recording temperature on TREK-1 current amplitude at +60 mV. (**B**) The potentiating effect of BL-1249 (30 µM) on TREK-1 current amplitude at different recording temperatures. (**C**, **D**) Representative traces of TREK-1 current (**C**) and quantification of current amplitude (**D**) after varying incubation periods of sodium butyrate (NaB, 3 mM) at 30°C. Recordings performed in multi-hole acquisition using a QPatch48 platform at 25°C. Data displayed as Mean ± SEM.

Robust TREK-1 activation by BL-1249 (i.e. >5-fold) across this temperature range was only detectable between 25°C and 30°C (Figure 2B), suggesting temperatures above 30°C elicit maximal open probability of TREK-1 channels. Increased temperatures cannot be reliably used to increase basal TREK-1 current amplitude due to the steep temperature dependence of the channel (and resulting variability in current amplitudes). Therefore, a temperature of 25°C was nominated as the optimal temperature and other methods of current enhancement were explored. Sodium butyrate (NaB) was assessed as an alternative means to boost overall TREK-1 channel expression. NaB treatment of CHO-TREK1 cells enhanced baseline current amplitude (recorded at 25°C) in a time-dependent manner, with increasing expression after 24 h and 48 h incubation (Figure 2C, D). Importantly, current amplitude in the presence of BL-1249 also increased with NaB treatment (nontreated, 5.05 ± 1.9 nA, mean ± SEM, n = 4; 24 h incubation, 11.52 ± 3.0 nA, mean ± SEM, n = 4; 48h incubation 27.48 ± 7.5 nA, mean ± SEM, n = 4). These results indicate that NaB enhances TREK-1 current amplitude by increased expression rather than shifted open probability. Using NaB to increase TREK-1 current amplitude ensures a sufficient assay window for both activators and inhibitors.

TREK-1 activity was examined on the Qube 384 to ensure compatibility with the QPatch48 results. TREK-1 currents and their responsiveness to BL-1249 on the Qube 384 mirrored activity on the QPatch48 (Figure 3a). Parental CHO cells were examined to ensure no contributing endogenous activity in the host cell line. No BL-1249 response was detected in CHO cells; however, a small outward current was detected at voltages above +20 mV. Therefore, current amplitudes were measured at +10 mV in subsequent experiments. The Qube 384 assay consisted of two vehicle additions: two compound additions of the same concentration, and a final BL-1249 addition to verify TREK-1 expression. TREK-1 currents were recorded for 3 min after each liquid addition (Figure 3B). Assessing the assay paradigm in the presence of vehicle (0.3 % v/v DMSO) demonstrated a stable response (Figure 3C).

BL-1249 demonstrated a concentration-dependent response against TREK-1 (Figure 4A) that was comparable in efficacy and potency to the QPatch 48 (Figure 4B), further supporting the viability of the assay paradigm.

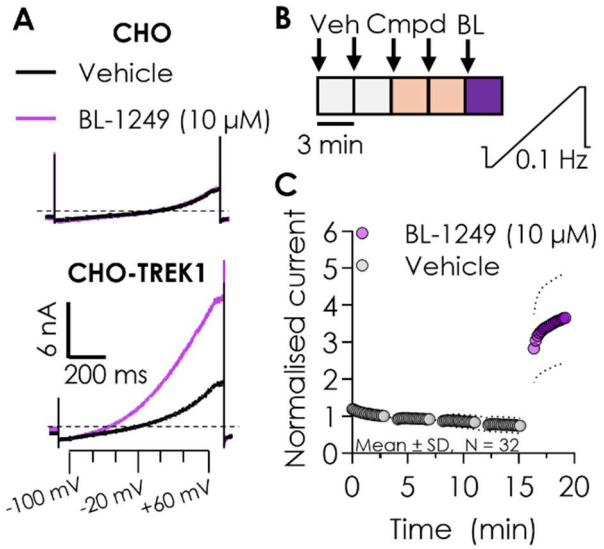


**Figure 3. TREK-1 assay development using Qube 384.** (**A**) Representative traces of CHO and CHO-TREK-1 cells in the presence and absence of BL-1249 (10 µM) following stimulation from -100 to +60 mV. (**B**) Assay paradigm for Qube 384 screening of TREK-1 activity. Each cell is exposed to two vehicle (Veh) additions, followed by two additions of a single concentration of compound or vehicle (Cmpd) and a final BL-1249 addition (BL, 10 µM). The standard voltage protocol (-100 to +60 mV ramp, 800 ms) is applied at 0.1 Hz. (**C**) Vehicle stability plot of TREK-1 current, current amplitude recorded at +10 mV. Recordings performed in multi-hole acquisition using a Qube 384 platform at 25°C.

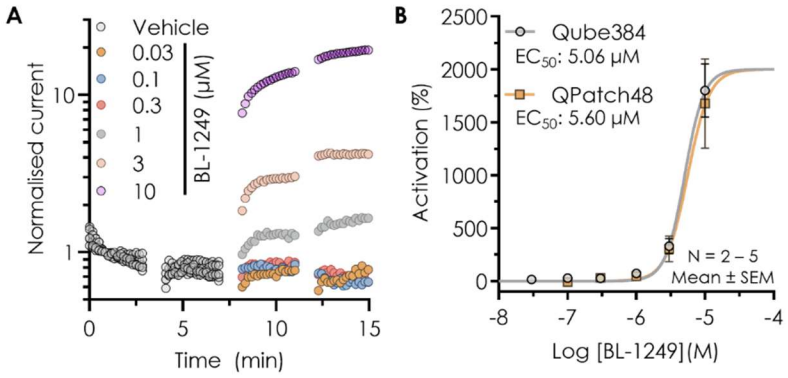


**Figure 4. Activation of TREK-1 current using BL-1249 on a Qube 384.** (**A**) BL-1249 activates TREK-1 at +10 mV in a concentration-dependent manner. A final BL-1249 application (10 μM) was used to verify current expression but has been truncated for clarity. Vehicle consisted of 0.3 % v/v DMSO. (**B**) Comparison of the potency and efficacy of BL-1249 activation of TREK-1 currents. Recordings performed in multi-hole acquisition using a Qube 384 platform at 25 °C. Data displayed as Mean ± SEM.

The Qube 384 assay was tested using a selection of different compounds with reported TREK-1 activity, including both activators and inhibitors. For instance, Amitriptyline demonstrated complete TREK-1 inhibition at 100 μM (Figure 5A) and BL-1249 demonstrated robust potentiation at 10 μM (Figure 5B). Representative current-time plots of a single concentration of each compound are displayed in Figure 5C. Concentration-response curves were plotted for each compound and $IC_{50}$s or $EC_{50}$s estimated (Figure 6A,B). Potency values aligned with literature values (Figure 6C), validating the assay paradigm and supporting its use in compound screening.

A library of ~600 peptides (Targeted Venom Discovery Array, provided by Venomtech, UK) was screened against TREK-1 on the Qube 384. Peptide activity was determined by measuring the change in current amplitude at +10 mV (Figure 7A).

A variety of peptides (derived from different taxa) produced a significant response, defined as a response greater than the mean vehicle response (+ 50 %) or smaller than the mean vehicle response (– 50 %) for activators and inhibitors, respectively. Representative traces for the most active peptides are displayed in figure 7B. Further studies will assess potency and selectivity of these peptides.

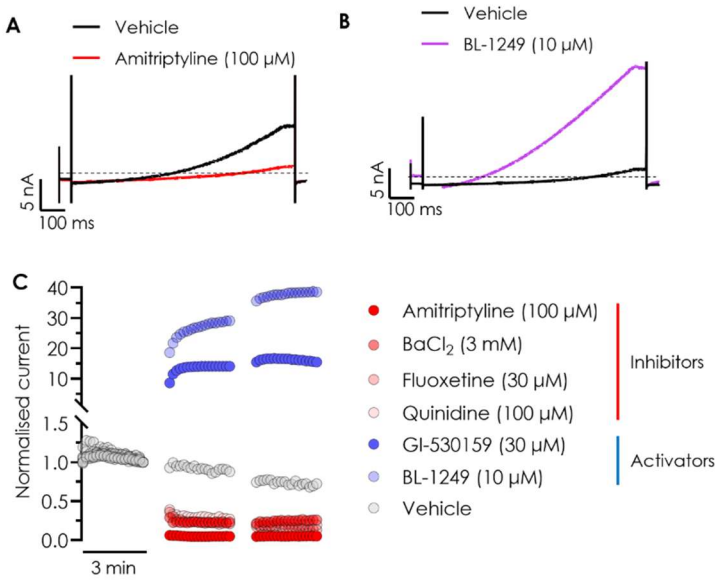


**Figure 5. Qube 384 screening of TREK-1 activity using reference compounds.** (**A**, **B**) Representative TREK-1 current traces in the presence and absence of Amitriptyline (**A**, 100 μM) and BL-1249 (**B**, 10 μM). (**C**) Current-time plot overlay of different CHO-TREK-1 cells exposed to various reference inhibitors, activators or vehicle. A final BL-1249 application was used to verify current expression but has been

truncated for clarity. Recordings performed in multi-hole acquisition using a Qube 384 platform at 25 °C.

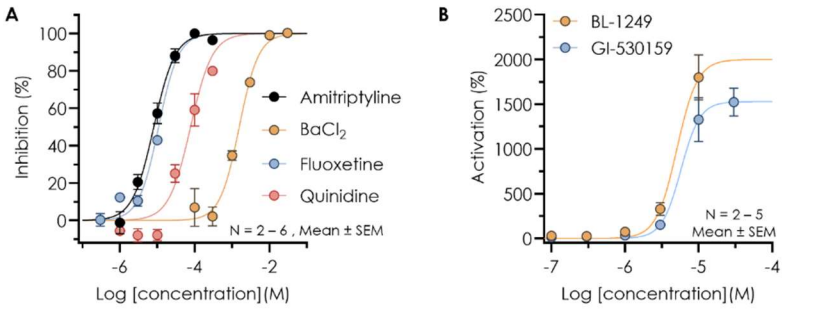


C

| Compound | $IC_{50}$ (µM) | $EC_{50}$ (µM) | Literature value (µM) |
|---|---|---|---|
| Amitriptyline | 8.08 | - | 16 (TREK-2[18]) |
| $BaCl_2$ | 1552 | - | 560[19] |
| Fluoxetine | 10.8 | - | 31 (TREK-2[18]) |
| Quinidine | 77.6 | - | 70 % at 200 µM[20] |
| BL-1249 | - | 5.06 | 7[16] |
| GI-530159 | - | 5.73 | 1[17] |

**Figure 6. Concentration response curves of reference compounds against TREK-1 activity from the Qube 384 assay.** (**A, B**) Concentration-response curves of different inhibitors (A) and activators (B). Data were fitted using a variable Hill slope, four-parameter curve. Curves were restraint between 0 – 100 % (inhibitors) or from 0 % (activators). (C) IC50 values derived from the concentration-response fits in A and B and corresponding IC50 values reported in the literature. Data displayed as Mean ± SEM.

## Conclusions

Metrion has developed a robust TREK-1 screening assay on the Qube 384 platform capable of identifying both activators and inhibitors of the TREK-1 channel. The optimized screening assay was employed in the successful screening of a venom library (Targeted Venom Discovery Array, Venomtech, UK) against TREK-1, detecting peptides with inhibitory and potentiating modalities.

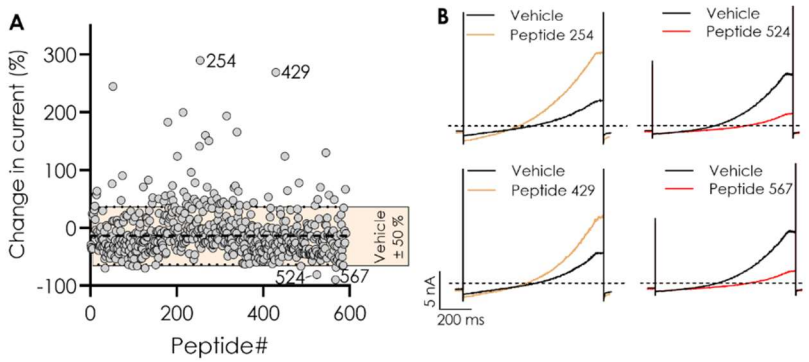


**Figure 7. Peptide screen of TREK-1 activity on Qube 384.** (**A**) TREK-1 activity was assessed using a peptide library and changes in current amplitude at +10 mV measured (**A**). A peptide was considered active if it induced a response greater than 50 % from the mean of the vehicle response (-13.7 %). Recordings performed in multi-hole acquisition using a Qube 384 platform at 25°C. (**B**) Representative traces of the two most active openers and inhibitors displayed.

## References


1. Goldstein SAN *et al.* (2005). International Union of Pharmacology. LV. Nomenclature and Molecular Relationships of Two-P Potassium Channels. Pharmacological Reviews December 2005, 57 (4) 527-540.
2. Fan X *et al.* (2022). Advances in the Understanding of Two-Pore Domain TASK Potassium Channels and Their Potential as Therapeutic Targets. Molecules. 2022 Dec; 27(23): 8296.
3. Andres-Bilbe A *et al.* (2020). The Background K+ Channel TRESK in Sensory Physiology and Pain. Int J Mol Sci. 2020 Jul 23;21(15):5206.
4. Lee EH *et al.* (2023). Novel potent blockers for TWIK-1/TREK-1 heterodimers as potential antidepressants. Biomed Pharmacother. 2023 Sep:165:115139.
5. Bauer CK *et al.* (2018). Mutations in KCNK4 that Affect Gating Cause a Recognizable Neurodevelopmental Syndrome. Am J Hum Genet 2018 Oct 4;103(4):621-630.
6. Prado PÁ *et al.* (2021). TREK channel activation suppresses migraine pain phenotype. iScience. 2021 Aug 8;24(9):102961.
7. Honoré E *et al.* (2007). The neuronal background K2P channels: focus on TREK1. Nat Rev Neurosci. 2007 Apr;8(4):251-61.
8. Natale AM *et al.* (2021). Structural Insights into the Mechanisms and Pharmacology of K2P Potassium Channels. J Mol Biol. 2021 Aug 20;433(17):166995.
9. Schewe M *et al.* (2016). A Non-canonical Voltage-Sensing Mechanism Controls Gating in K2P K+ Channels. Cell. 2016 Feb 25;164(5):937-49.
10. Honoré E *et al.* (2006). Desensitization of mechano-gated K2P channels. Proc Natl Acad Sci U S A. 2006 May 2;103(18):6859-64.
11. Maingret F *et al.* (2000). Lysophospholipids Open the Two-pore Domain Mechano-gated K(+) Channels TREK-1 and TRAAK. J Biol Chem. 2000 Apr 7;275(14):10128-33.
12. Chemin J *et al.* (2005). A phospholipid sensor controls mechanogating of the $K^+$ channel TREK-1. EMBO (2005) 24, 44–53.
13. Maingret F *et al.* (2000). TREK-1 is a heat-activated background K(+) channel. EMBO J. 2000 Jun 1;19(11):2483-91.
14. Blin S *et al.* (2014). Tandem pore domain halothane-inhibited K+ channel subunits THIK1 and THIK2 assemble and form active channels. J Biol Chem. 2014 Oct 10;289(41):28202-12.
15. Decher N *et al.* (2021). Molecular Pharmacology of K2P Potassium Channels. Cell Physiol Biochem 2021;55(S3):87-107.
16. Pope L *et al.* (2018). Protein and Chemical Determinants of BL-1249 Action and Selectivity for K2P Channels. ACS Chem Neurosci 2018 Dec 19;9(12):3153-3165.
17. Loucif AJC *et al.* (2018). GI-530159, a novel, selective, mechanosensitive two-pore-domain potassium (K2P ) channel opener, reduces rat dorsal root ganglion neuron excitability. Br J Pharmacol 2018 Jun;175(12):2272-2283.
18. Park H *et al.* (2016). Effects of analgesics and antidepressants on TREK-2 and TRESK currents. Korean J Physiol Pharmacol 2016;20(4):379-385.
19. Ma X-Y *et al.* (2011). External $Ba2^+$ Block of the Two-pore Domain Potassium Channel TREK-1 Defines Conformational Transition in Its Selectivity Filter. J Biol Chem. 2011 Nov 18;286(46):39813-22.
20. Bae Y *et al.* (2020). Spadin Modulates Astrocytic Passive Conductance via Inhibition of TWIK-1/TREK-1 Heterodimeric Channels. Int J Mol Sci. 2020 Dec 17;21(24):9639.